Astron. Astrophys. 234, 447–453 (1990)

ASTRONOMY AND ASTROPHYSICS

Morphology and kinematics of the molecular cloud associated with GM 24 ⋆

J.F. Gómez [1], J.M. Torrelles [1], M. Tapia [2], M. Roth [3], L. Verdes-Montenegro [1], and L.F. Rodríguez [4]

[1] Instituto de Astrofísica de Andalucía, Apdo. Correos 2144, E-18080 Granada, Spain
[2] Instituto de Astronomía, Universidad Nacional Autónoma de México, Apdo. Postal 877, 22830 Ensenada, B.C., México
[3] Las Campanas Observatory, Carnegie Institution of Washington, Casilla 601, La Serena, Chile
[4] Instituto de Astronomía, Universidad Nacional Autónoma de México, Apdo. Postal 70-264, 04510 México, D.F., México

Received November 6, 1989; accepted January 16, 1990

Abstract. We have observed the CO ($J=2\rightarrow1$), ^{13}CO ($J=1\rightarrow0$) and C^{18}O ($J=1\rightarrow0$) rotational transition lines toward the star formation region associated with GM 24 using the SEST. The optical nebulosity GM 24 was suspected to be the outer part of a previously reported blister type H II region expanding mainly toward the north. We find a broadening of the C^{18}O and ^{13}CO linewidths near the blister H II region, implying a perturbation of the molecular gas by the action of the star formation and/or the presence of systematic motions unresolved by our beam. These motions probably are of expansive character and result from the presence of a young, massive star or stars. The C^{18}O emission shows, to the north, a clumpy molecular structure. The C^{18}O clumps are mainly distributed toward the north-east and north-west directions. The ^{13}CO emission presents a similar structure, but with a weaker southern counterpart.

We consider whether the C^{18}O and ^{13}CO structures existed before the star formation took place or was produced by the star formation processes. In particular, we suggest that the clumpy structures may delineate the walls of a molecular cavity, evacuated by the expanding motions of a faint and extended ionized component of the observed blister H II region during an evolution time of $\sim10^5$ yr. New VLA radio continuum observations covering short spacings can test this interpretation.

Key words: interstellar medium: molecules – H II regions

1. Introduction

Many emission nebulosities associated with extremely young clusters of massive stars have been found to exhibit characteristics of *blister* H II regions. These ionized gas structures are density bounded towards the external parts of the molecular cloud, that is starting to be broken by the ionization produced by the recently formed massive stars, while they are ionization bounded towards the inside of the cloud. The gas presents a velocity gradient in the direction of the flow and its density decreases exponentially as it streams away from the cloud. For a recent review, see Yorke (1986).

The region of recent star formation associated with GM 24 (or PP 85, see Parsamian and Petrosian, 1979) seems to be a good example of this phenomenon. First observed in a CO survey of peculiar nebulosities made by Torrelles et al. (1983), it was selected for further detailed studies since its high antenna temperature was suggestive of recent massive star formation. On energetic arguments, Torrelles et al. (1983) suggested that the gas and dust in the region should be heated by at least one embedded O type star, consistent with the presence of a far infrared and radio continuum source at roughly the same position in the sky. In particular, 6 cm continuum observations, carried out by Altenhoff et al. (1970) using the 140 ft antenna of Green Bank, show an extended ($\sim15'\times8'$) H II region (RCW 126) with a total flux of 9 Jy, which is apparently related to GM 24.

Tapia et al. (1985) performed a near-infrared survey, detecting the presence of a cluster of at least five luminous stars deeply embedded (with A_V of up to 65 mag) in the molecular cloud. One of these (Irs 3) coincided with the peak of a bright H II region and with the center of the CO hot spot. The infrared cluster has dimensions of around 50″ in diameter which corresponds to about 0.5 pc at the assumed kinematic distance to GM 24 of 2 kpc (Torrelles et al., 1983). This distance is similar to that of other nearby star formation regions found toward the Sagittarius region, for example, NGC 6334. Recent high resolution infrared images (Tapia et al., 1989) reveal the presence of more than 20 other lower luminosity members of the embedded cluster.

The shape and kinematics of the H II region, as studied through 2 cm continuum and line (H 76α) emission VLA observations (beam size $\simeq1''$) by Roth et al. (1988), led these authors to suggest that GM 24 is a *blister* H II region extending over 15″ that has bursted out of its parent molecular cloud and is passing through its *champagne* phase (e.g., Yorke et al., 1983). In agreement with the characteristics of this model, Roth et al. (1988) found a north-south radial velocity gradient of ~6–$8\,\mathrm{km\,s^{-1}}$ over 0.1 pc, together with a relative sharp decrease in the radio continuum emission to the south and a much smoother emission distribution to the north.

Send offprint requests to: J.F. Gómez

⋆ Based on observations collected at the European Southern Observatory, La Silla, Chile

In the present work, new high resolution observations in the CO ($J=2\rightarrow1$), ^{13}CO ($J=1\rightarrow0$), and C^{18}O ($J=1\rightarrow0$) lines of the molecular cloud associated with GM 24 are presented. The aim of this work is to determine the morphology, kinematics and excitation structure of the cloud in order to test the applicability of the *blister* H II region models to GM 24.

2. Observations

We observed the CO ($J=2\rightarrow1$), ^{13}CO ($J=1\rightarrow0$) and C^{18}O ($J=1\rightarrow0$) rotational transition lines by using the 15-m Swedish-European Submillimeter Telescope (SEST) at La Silla, Chile, during 14–16 March, 1989. At the observing frequencies of $\sim$230 (CO) and $\sim$110 (^{13}CO, C^{18}O) GHz, the Half Power Beam Width (HPBW) of the telescope is $\sim$22″ and 46″, respectively. We used two Schottky receivers with two acousto-optic spectrometers, one covering a bandwidth of 100 MHz and spectral resolution of 50 kHz ($\sim$0.14 km s^{-1} for the 110 GHz observations), and the other one covering a bandwidth of 500 MHz and spectral resolution of 1 MHz ($\sim$1.3 km s^{-1} for the 230 GHz observations). Detailed information on the SEST system can be found in Booth et al. (1987). The rms pointing error of the telescope was $\sim$8″. Typical system temperatures of $T_{sys}^{*}\sim400$ K and 1500 K at 110 and 230 GHz were obtained, respectively. The 110 GHz observations were made by using the frequency switching mode, while position switching mode was used for the 230 GHz observations. We mapped an area of $\sim100''\times100''$ in the CO ($J=2\rightarrow1$) line, and an area of $\sim200''\times200''$ in the ^{13}CO ($J=1\rightarrow0$) and C^{18}O ($J=1\rightarrow0$) lines. All the maps were centered on the position of the H II region given by Tapia et al. (1985): $\alpha(1950)=17^{h}13^{m}40^{s}.3$, $\delta(1950)=-36°17'56''$. The offset positions of the maps shown in this paper are given in arcsec with respect to that central position.

Figure 1 shows the observed CO ($J=2\rightarrow1$), ^{13}CO ($J=1\rightarrow0$), and C^{18}O ($J=1\rightarrow0$) spectra toward the central position. CO intensities are given in unities of T_A^* (K) (Ulich and Haas, 1976). The CO spectrum shows blueshifted line wing emission at a level of $T_A^*\simeq0.5$ K. Because of the weakness of the signal of this high-velocity emission, we did not attempt to map it. In Fig. 2 we show a contour map of the peak antenna temperature (T_A^*) of the CO line. This map peaks $\sim$30″ north-west of the central position, reaching a value of $T_A^*\simeq34$ K. Contour maps of the integrated intensity $\int T_A^*\,dv$ (K km s^{-1}) over the velocity range $V_{LSR}=-20\rightarrow-6$ km s^{-1} of the C^{18}O and ^{13}CO lines are shown in Figs. 3 and 4, respectively.

The C^{18}O emission (Fig. 3) reveals a clumpy molecular gas structure. The molecular gas is mainly concentrated from the central position toward the north-east and north-west directions. There is a relative decrease of C^{18}O emission along the north-south and east-west directions. The ^{13}CO map (Fig. 4) shows, in the northern region, a structure similar to the C^{18}O one, with protuberances of emission also extending toward the north-east and north-west directions. There is, however, a southern ^{13}CO weaker counterpart of that stucture, which is not detected in C^{18}O. We have also detected ^{13}CO emission at $V_{LSR}=-3.5$ km s^{-1}. Nevertheless, this emission was not fully mapped by

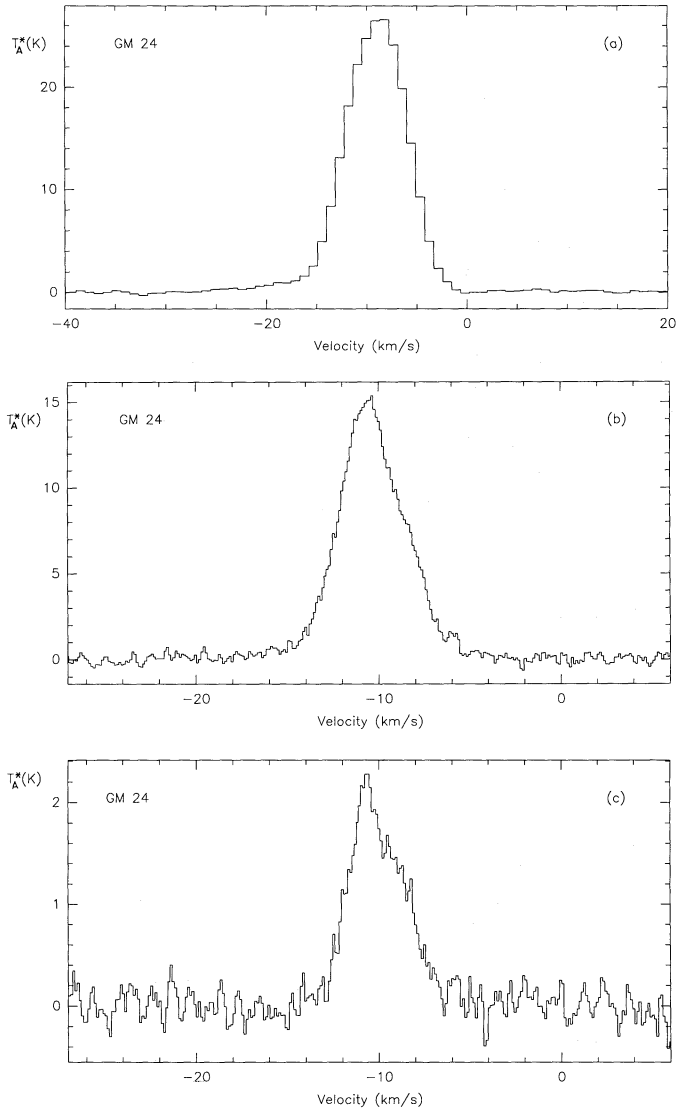

Fig. 1a–c. Observed spectra of the ^{12}CO ($J=2\rightarrow1$) (**a**), ^{13}CO ($J=1\rightarrow0$) (**b**) and C^{18}O ($J=1\rightarrow0$) (**c**) lines toward the (0,0) position offset ($\alpha(1950)=17^{h}13^{m}40^{s}.3$, $\delta(1950)=-36°17'56''$). Horizontal axis represents the V_{LSR}

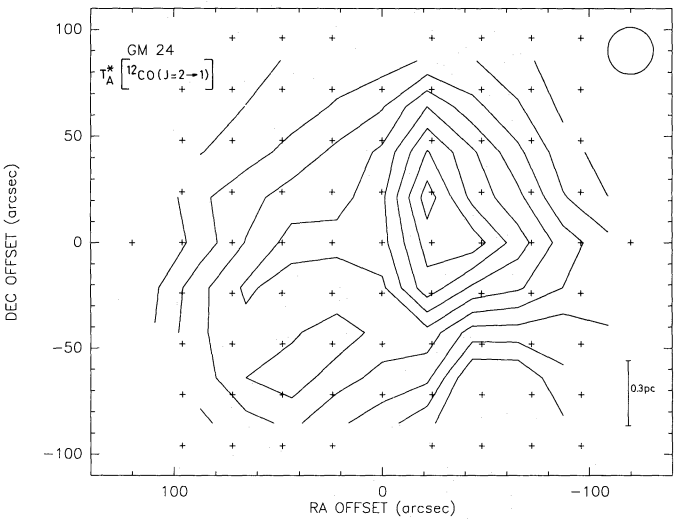

Fig. 2. Contour map of the ^{12}CO ($J=2\rightarrow1$) line peak antenna temperature (T_A^*). Contour levels are 18, 20, 22, 24, 26, 28, 30, 32, and 34 K. The crosses indicate the observed points and the circle is the HPBW

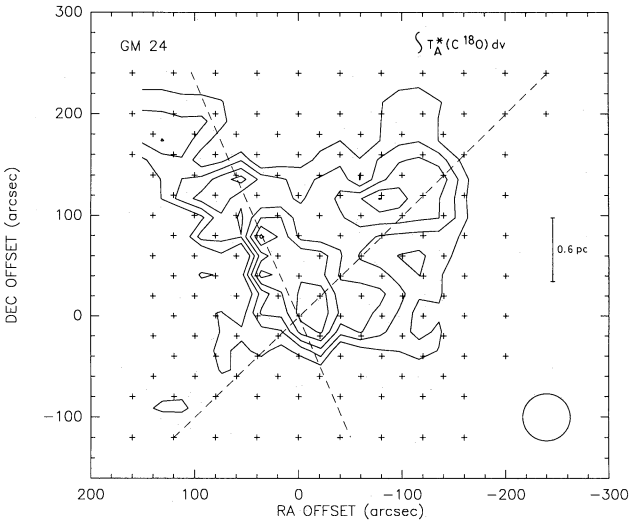

Fig. 3. Contour map of the $C^{18}O$ ($J=1\rightarrow0$) emission, integrated over the velocity range $V_{LSR}=-20\rightarrow-6\,km\,s^{-1}$. Contour levels are 3, 4, 5, 6, 7, and 8 K km s^{-1}. We identify five condensations, centered at (0″, 0″), (40″, 80″), (60″, 120″), (140″, 180″), and (−80″, 120″). Dashed lines indicate the direction along which position velocity diagrams are constructed (see Fig. 6)

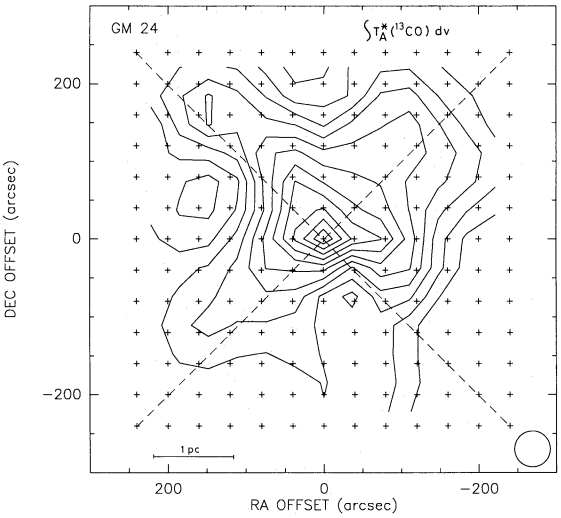

Fig. 4. Contour map of the ^{13}CO ($J=1\rightarrow0$) emission, integrated over the velocity range $V_{LSR}=-20\rightarrow-6\,km\,s^{-1}$. The lowest contour is 10 K km s^{-1} and the increment step is 5 K km s^{-1}. Dashed lines indicate the direction along which position velocity diagrams are constructed (see Fig. 6)

our observations as it is located ∼230″ north-west and ∼200″ south of the central position. Since this emission seems not to be related with the stellar activity center, we will refrain from discussing it.

In Table 1 we give the Gaussian fit parameters of the observed CO, ^{13}CO and $C^{18}O$ spectra toward the central positions of the $C^{18}O$ clumps (see Fig. 3). The CO peak velocities are different from those of the ^{13}CO and $C^{18}O$, probably because of opacity effects. We give in Table 2 the physical parameters of the $C^{18}O$ clumps: opacity (τ), column density [$N(cm^{-2})$], abundance [$\tau(^{13}CO)/\tau(C^{18}O)$], size [$\theta$(″)], mass [$M(M_\odot)$], and visual extinction [A_V(mag)]. These parameters were obtained as indicated in the footnotes to Table 2. The $C^{18}O$ emission is optically thin, with typical opacities of ∼0.1 and $\tau(^{13}CO)/\tau(C^{18}O)$ ratios of ∼5–10. This is probably the reason for the non-detection in $C^{18}O$ of the weak southern structure observed in ^{13}CO, as the limit of the expected $C^{18}O$ integrated intensity in the southern region (obtained from the observed ratio of ^{13}CO and $C^{18}O$ in the northern region) is $\leqq 3$ K km s^{-1}, similar to our $C^{18}O$ sensitivity level. From the $C^{18}O$ data we estimate a total mass of $\sim 4\,10^3\,M_\odot$ for the molecular cloud, an average volume density $n(H_2)$ of a *few* times 10^4 cm^{-3}, and a visual extinction, A_V, in the ∼50–90 mag range. These extinctions are similar to those inferred by Tapia et al. (1985) from near-infrared observations. Assuming an internal velocity dispersion of ∼3 km s^{-1} (from the $C^{18}O$ linewidths, see Table 1) and a radius of ∼1 pc for the molecular cloud as a whole, we estimate a virial mass of $\sim 2\,10^3\,M_\odot$, similar to the observed molecular mass ($\sim 4\,10^3\,M_\odot$). Therefore, we conclude that the molecular cloud is in approximate virial equilibrium.

From the $C^{18}O$ and ^{13}CO opacities (Table 2) we derive an abundance $[N(^{13}CO)/N(C^{18}O)] \simeq 5$–10 for the GM 24 molecular cloud. These abundances are similar to those obtained by Frerking et al. (1982) in the ρ Ophiuchi and Taurus molecular clouds. We must also note that our estimated column densities of H_2 and $C^{18}O$ (Table 2) fit well to the empirical correlation of $N(H_2)$ on $N(C^{18}O)$ obtained by Frerking et al. (1982) in ρ Ophiuchi and Taurus for dense cores [$N(C^{18}O) \geqq 3\,10^{14}$ cm^{-2}] by measuring the visual extinction of field stars. This fact implies that, at least in terms of abundances of CO and its isotopic species, the GM 24 molecular cloud has similar characteristics to these two regions.

3. Discussion

There is a velocity gradient along the north-south direction of ∼1 km s^{-1} pc^{-1} as measured by the peak center of the CO line (Fig. 5). The velocities increase from north to south; therefore, with the same sign as the velocity gradient of ∼70 km s^{-1} pc^{-1} observed by Roth et al. (1988) at scales of ∼10″ in the GM 24 blister H II region.

In Fig. 6 we show several position velocity diagrams of the $C^{18}O$ (Fig. 6, top) and ^{13}CO (Fig. 6, bottom) emission along the

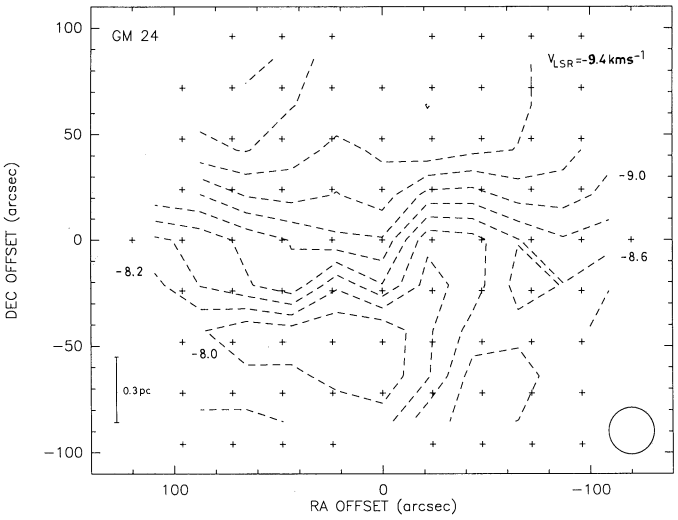

Fig. 5. Contour map of the ^{12}CO ($J=2\rightarrow1$) peak velocity measured by Gaussian fits to the observed spectra. Contour levels are indicated in the figure

Table 1. Line parameters[a] at the positions of the $C^{18}O$ clumps

Offset (arcsec)	CO			^{13}CO			$C^{18}O$		
	T_A^* (K)	V_{LSR} (km s^{-1})	ΔV (km s^{-1})	T_A^* (K)	V_{LSR} (km s^{-1})	ΔV (km s^{-1})	T_A^* (K)	V_{LSR} (km s^{-1})	ΔV (km s^{-1})
(0, 0)	27.3±0.6	−8.98±0.04	7.00±0.10	14.4±0.6	−10.43±0.01	4.18±0.02	1.99±0.17	−10.20±0.04	3.60±0.09
(40, 80)	20.5±0.4	−9.64±0.03	5.39±0.07	12.7±0.3	−11.16±0.01	3.09±0.02	3.43±0.10	−11.31±0.02	2.19±0.04
(60, 140)[b]	–	–	–	8.3±0.7	−10.84±0.02	3.06±0.06	2.05±0.21	−10.88±0.05	2.60±0.14
(140, 180)[b]	–	–	–	7.4±0.7	−10.15±0.03	3.76±0.08	1.09±0.15	−10.38±0.15	4.74±0.38
(−80, 120)[b]	–	–	–	10.5±0.5	−10.73±0.02	2.91±0.04	2.57±0.23	−10.92±0.03	2.20±0.07

[a] Obtained from Gaussian fits to the CO, ^{13}CO and $C^{18}O$ spectra.
[b] These positions were not mapped in CO (see Fig. 2).

Table 2. Physical parameters of the observed $C^{18}O$ clumps

Offset (arcsec)	T_K[a] (K)	$\tau(^{13}CO)$[b]	$\tau(C^{18}O)$[b]	$\int T_A^*(^{13}CO)\,dV$ (K km s^{-1})	$\int T_A^*(C^{18}O)\,dV$ (K km s^{-1})	$N(^{13}CO)$[c] (10^{16} cm^{-2})	$N(C^{18}O)$[c] (10^{16} cm^{-2})	$\tau(^{13}CO)/\tau(C^{18}O)$	$N(H_2)$[d] (10^{22} cm^{-2})	$\theta_a \times \theta_b$[e] (arcsec)	M[f] ($M_\odot$)	A_V[g] (mag)
(0, 0)	35.1	0.68	0.07	64.0	7.6	12.0	1.4	9.6	8.9	100 × 145	1500	89
(40, 80)	27.6	0.85	0.17	41.9	8.0	6.5	1.2	5.0	7.7	70 × 65	400	77
(60, 140)	27.1[h]	0.48	0.10	27.5	5.7	4.2	0.9	4.9	5.4	65 × 45	200	54
(140, 180)	27.1[h]	0.42	0.05	29.6	5.5	4.6	0.8	8.1	5.2	95 × 140	800	52
(−80, 120)	27.1[h]	0.66	0.13	32.4	6.0	5.0	0.9	5.2	5.7	115 × 140	1100	57

[a] Kinetic temperature obtained from $T_R^*(CO) = T_A^*(CO)/\eta_{fss}$, where η_{fss} is the forward spillover and scattering efficiency of the telescope (Kutner and Ulich, 1981) ($\eta_{fss} = 0.92$ for the SEST).
[b] Optical depths, obtained from the radiative transfer equation assuming $T_{ex}(C^{18}O) = T_{ex}(^{13}CO) = T_K$, and filling factor of unity.
[c] Column densities obtained via the optically thin emission approximation $N = 5.5\ 10^{14} \dfrac{Q \int T_R^*\,dV\,(\mathrm{K\,km\,s^{-1}})}{[J(T_{ex}) - 0.87]\,[1 - \exp(-5.27/T_{ex})]}\,\mathrm{cm^{-2}}$, where $J(T) = \dfrac{h\nu/k}{\exp(h\nu/kT) - 1}$, and Q is the partition function.
[d] Hydrogen column densities, assuming abundances $^{13}CO/C^{18}O \simeq 7$ (from the observed $\tau(^{13}CO)/\tau(C^{18}O)$ ratio, this paper), $CO/^{13}CO \simeq 89$ (terrestrial ratio), and $H_2/CO \simeq 10^4$ (Herbst and Leung, 1989).
[e] Angular size of the FWHM of the $C^{18}O$ emission.
[f] Mass of the clumps. A projected area of πr^2, where $r = \frac{1}{2}(\theta_a \theta_b)^{1/2}$, has been adopted.
[g] $(A_V/\mathrm{mag}) \simeq 10\ (N(H_2)/10^{22}\,\mathrm{cm^{-2}})$ (Spitzer, 1978).
[h] A $T_A^*(CO) = 20$ K has been assumed for these positions, where CO observations are not available (see Table 1 and Fig. 2).

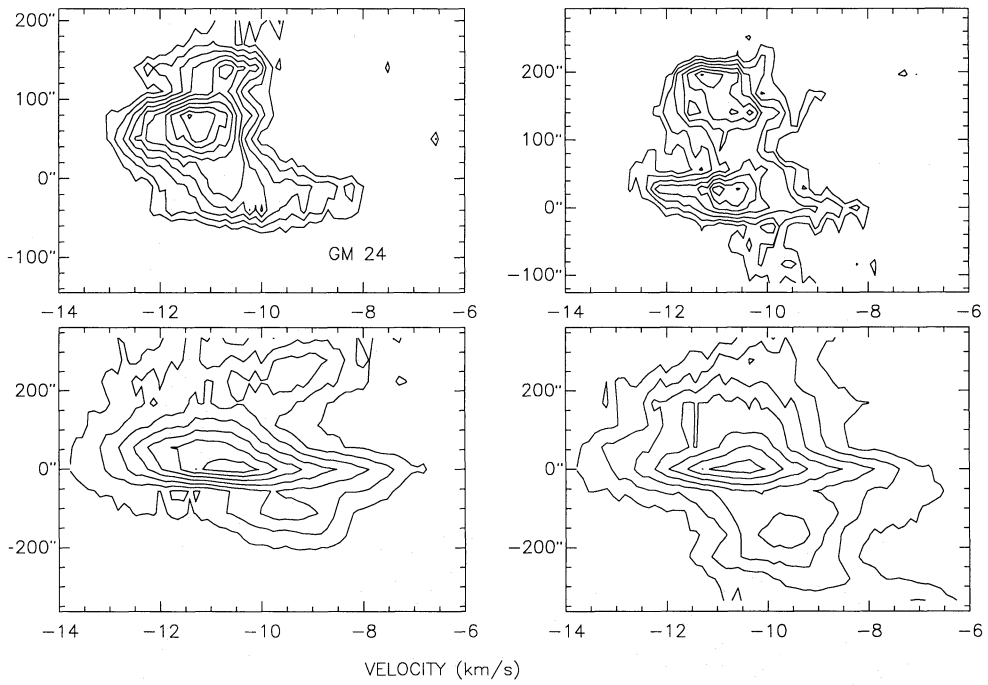

Fig. 6. Position velocity diagrams for the $C^{18}O$ ($J=1\rightarrow0$) along the axes with p.a. = 23° (*top left*) and −45° (*top right*) (see Fig. 3), as well as for the ^{13}CO ($J=1\rightarrow0$) along p.a. = 45° (*bottom left*) and −45° (*bottom right*) (see Fig. 4). Lowest contours are 0.8 K for the $C^{18}O$ ($J=1\rightarrow0$) and 2 K for the ^{13}CO ($J=1\rightarrow0$), with increment steps of 0.3 and 2 K, respectively. Spatial coordinate in arcsec (vertical axis) is with respect to the (0,0) position

axes with position angles (north to east) p.a. = 23° and −45° ($C^{18}O$), and 45° and −45° (^{13}CO) through the central position. We have selected these p.a. since they contain most of the molecular clumps. There is evidence of a perturbation of the molecular gas near the stellar activity center, as it is traced by the significant enhancement of the $C^{18}O$ and ^{13}CO linewidths at that position. In particular, the $C^{18}O$ velocity position diagrams (Fig. 6, top) show a half power width emission extending over $\sim 3.6\,km\,s^{-1}$ near the central position, while at ∼80″ and 140″ north-east of the stellar activity center the emission is extending over ~ 2.2 and $2.6\,km\,s^{-1}$ (see also linewidths in Table 1). A similar behaviour is observed in ^{13}CO (Fig. 6, bottom, Table 1). Since we have found that these rotational transition lines, specially the $C^{18}O$ ones, are optically thin (Table 2), we attribute those enhancements to local turbulence and/or systematic motions associated to the star forming region unresolved by our beam, with a lower perturbation of the molecular gas far from the stellar activity center.

We find also broad linewidths at (140″, 180″), with values of $\Delta V(C^{18}O) \simeq 4.7\,km\,s^{-1}$ and $\Delta V(^{13}CO) \simeq 3.8\,km\,s^{-1}$ (Table 1). Unfortunately, these broad lines are located at the border of our mapped region, making difficult to study this possible perturbation of the molecular gas at that position.

In Fig. 7 we show the contour map of the $C^{18}O$ integrated intensity (Fig. 3) and, as a close up of the central region, the contour map at 2 cm of the blister H II region obtained by Roth et al. (1988) superposed on a CCD Hα image of the GM 24 nebula (Tapia et al., 1989). This blister H II region was interpreted by Roth et al. (1988) as undergoing the champagne phase toward the north direction, producing a velocity gradient across the face of the H II region. These authors also concluded that the cometary optical nebula GM 24, which seems to be connected with the H II region and extends ∼20″ to the north, is probably the visible part of the H II region.

Our observations point to two possible interpretations. The first of them is that the observed $C^{18}O$ structure was created before the star formation process began. In fact, the alignment of the $C^{18}O$ clumps in the north-east direction is parallel to the galactic plane, where concentration of a greater amount of gas is favored. In this case, the north-western $C^{18}O$ gas, that is mainly concentrated on (−80″, 120″), would be an isolated clump, without any structural relationship with the other ones (see Fig. 7). These initial conditions of the molecular gas distribution around the stellar activity center, with an original relative decrease of gas along the north-south direction, would favor the expansion of the H II region toward that direction. This could explain the observed morphology and kinematics of the blister H II region (Fig. 7). There is, however, a main difficulty for this interpretation. Our ^{13}CO map shows (Fig. 4), as it was mentioned in Sect. 2, a structure with similar morphology to that of the $C^{18}O$ one, but with a weaker southern counterpart. We think it is difficult that this symmetry grows up only under the influence of the galactic plane.

The second possible interpretation is that the observed clumpy molecular structure has been created by the expanding motions of the H II region, sweeping the molecular gas mainly along the north direction and depositing it at both sides of the expanding H II region. Thus, the observed molecular gas located toward the north-east and north-west directions would represent the walls of a cavity in the molecular cloud, disrupted by the action of the expanding motions of the blister H II region. The main problem with this interpretation is that the size of the observed blister H II region is apparently too small (∼15″) to create a cavity of ∼2′, as observed in the $C^{18}O$ structure (see Fig. 7). However, we think that sensitivity and lack of short spacings in the VLA observations of the H II region may have suppressed the extended components in the continuum emission map. At a typical expansion velocity of $10\,km\,s^{-1}$, the H II region could fill a cavity with 1 pc (∼100″) of radius in 10^5 yr. This time scale is compatible with the estimated age for the GM 24 nebula ($\geqq 10^5$ yr, Tapia et al., 1985). This radius is similar to the size of the proposed molecular cavity. Considering pressure equilibrium between the ionized and molecular gas at a distance of 100″, with a molecular kinetic temperature and hydrogen volume density of 30 K and $10^4\,cm^{-3}$, respectively, we

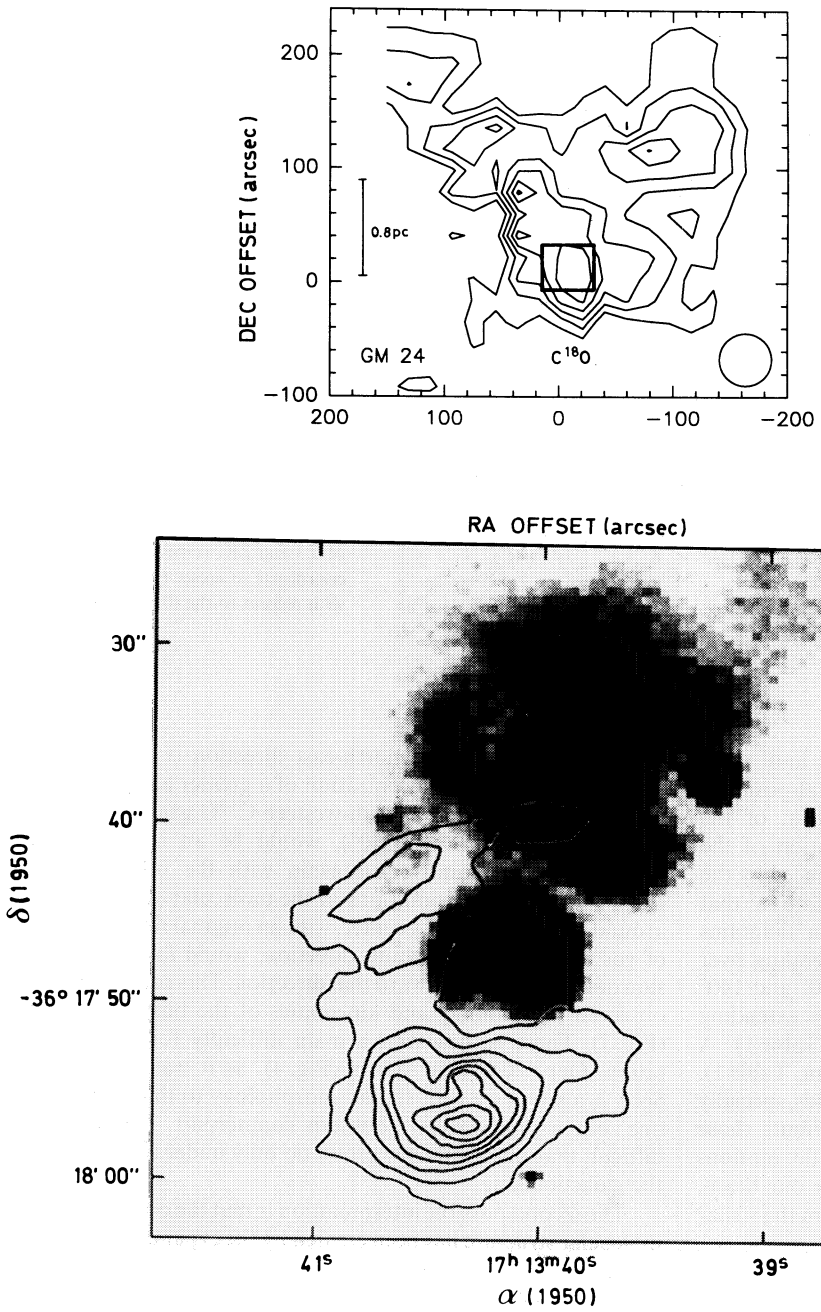

Fig. 7. 2-cm continuum contour map (Roth et al., 1988) superposed on a CCD Hα image of the GM 24 nebula (Tapia et al., 1989) as a close up of the $C^{18}O$ ($J=1\rightarrow0$) integrated intensity map (Fig. 3). Box in the $C^{18}O$ ($J=1\rightarrow0$) map indicates the size of the CCD Hα image

find that an electron density of $\sim 15\,cm^{-3}$ is enough to support the molecular cavity. The expected continuum flux at $\lambda = 2$ cm (see Rodríguez et al., 1980) for such an extended (radius = 100″) H II region, when observed with a beam size of 1″, is $S_\nu(\lambda = 2\,cm) \sim 10^{-3}$ mJy/beam. This flux is much lower than the sensitivity reached by the 2 cm continuum observations carried out by Roth et al. (1988) (rms $\simeq$ 1 mJy/beam). This would explain its non detection by previous VLA continuum observations. However, we speculate whether this proposed faint and extended H II region is related to the extended ($\sim 15' \times 8'$) 6 cm continuum source detected by Altenhoff et al. (1970).

Within this proposed model, the observed weak blueshifted CO wings (see Fig. 1) may have been also produced by the expanding motions of the H II region. Finally, it should be mentioned that the presence in ^{13}CO of a weak southern structure could imply some expanding motions of the H II region also toward the south direction.

We think that to clarify the interaction of the expanding motions of the H II region with the molecular gas, new more sensitive VLA radio continuum observations covering short spacings in the (u, v) plane will be needed. These will define better the morphology and extension of the faint and extended blister H II region. In particular, these new proposed observations may reveal whether the blister H II region covers the GM 24 optical nebula, as well as reveal if there is radio continuum emission toward the south direction as suggested by the ^{13}CO structure.

4. Conclusions

We have observed the molecular cloud associated with GM 24 in the rotational transition lines of CO ($J=2\rightarrow1$), ^{13}CO ($J=1\rightarrow0$), and $C^{18}O$ ($J=1\rightarrow0$). Our main conclusions can be summarized as follows.

There is a significant enhancement of the $C^{18}O$ and ^{13}CO linewidths near the stellar activity center. This implies interaction of the star formation with the molecular gas and/or systematic motions unresolved by our beam. We derive an abundance $[^{13}CO/C^{18}O] \simeq 7$ for the GM 24 molecular cloud. The characteristics of this cloud, in terms of abundances of CO and its isotopic species, are similar to those of ϱ Ophiuchi and Taurus.

We observed in $C^{18}O$ a northern clumpy molecular structure. The ^{13}CO structure is similar to the $C^{18}O$, but with a weaker southern counterpart. We argue that this structure may delineate the walls of a cavity created in the molecular gas by an expansion of the blister H II region toward the northern region in an evolution time of $\sim 10^5$ yr. The presence of the ^{13}CO southern weak counterpart suggests that some expanding motions of the H II region could be also present toward the south direction. These expanding motions would be also responsible for the weak blueshifted line wing emission observed toward the central position, as well as the CO velocity gradient in the north-south direction. In this model, a faint and extended ($\sim 100''$) ionized component of the blister H II region is expected to be filling the proposed molecular cavity. New VLA radio continuum observations covering short spacings can test this interpretation.

Acknowledgements. We would like to thank Jorge Cantó for a careful reading of the manuscript and helpful comments. We would like also to thank our anonymous referee for the helpful comments which have helped our paper. We acknowledge the hospitality offered to JFG, JMT, and LV by the IRAM (Granada, Spain) during part of the data reduction. JMT acknowledges the hospitality offered by the Instituto de Astronomía (UNAM, Ensenada, México) during the preparation of this paper. JFG, JMT, and LV, are supported in part by SEUI (Spain) grant PB 87-0371, and by Junta de Andalucía (Spain).

References

Altenhoff, W.J., Downes, D., Goad, L., Maxwell, A., Rinehart, R.: 1970, *Astron. Astrophys. Suppl.* **1**, 319

Booth, R.S., de Jonge, M.J., Shaver P.A.: 1987, *The Messenger* **48**, 2

Frerking, M.A., Langer, W.D., Wilson, R.W.: 1982, *Astrophys. J.* **262**, 590

Herbst, E., Leung, C.M.: 1989, *Astrophys. J. Suppl.* **69**, 271

Kutner, M., Ulich, B.L.: 1981, *Astrophys. J.* **250**, 341

Parsamian, E.S., Petrosian, V.M.: 1979, *Soobshemia Biurakanskoi Observatori, Akad. Nauk. Armianskoi S.S.R.*, No. 51

Rodríguez, L.F., Moran, J.M., Ho, P.T.P., Gottlieb, E.W.: 1980, *Astrophys. J.* **235**, 845

Roth, M., Tapia, M., Gómez, Y., Rodríguez, L.F.: 1988, *Rev. Mex. Astron. Astrof.* **16**, 3

Spitzer, L.: 1978, in *Physical Processes in the Interstellar Medium*, Wiley, New York

Tapia, M., Roth, M., Rodríguez, L.F., Cantó, J., Persi, P., Ferrari-Toniolo, M., López, J.A.: 1985, *Rev. Mex. Astron. Astrof.* **11**, 83

Tapia, M., Roth, M., Rodríguez, L.F.: 1989, *Rev. Mex. Astron. Astrof.* **18**, 177

Torrelles, J.M., Rodríguez, L.F., Cantó, J., Marcaide, J., Gyulbudaghian, A.L.: 1983, *Rev. Mex. Astron. Astrof.* **8**, 147

Ulich, B.L., Haas, R.W.: 1976, *Astrophys. J. Suppl.* **30**, 247

Yorke, H.W.: 1986, *Ann. Rev. Astron. Astrophys.* **24**, 49

Yorke, H.W., Tenorio-Tagle, G., Bodenheimer, P.: 1983, *Astron. Astrophys.* **127**, 313